



# Evaporation-driven self-assembly in the mixtures of micro and nanoparticles

RAVI KUMAR PUJALA<sup>1</sup>, DEVIKA VENKUZHY SUDHAKARAN<sup>2</sup>  and SURAJIT DHARA<sup>2,\*</sup> 

<sup>1</sup>Soft and Active Matter Group, Department of Physics, Indian Institute of Science Education and Research (IISER), Tirupati, Andhra Pradesh 517507, India

<sup>2</sup>School of Physics, University of Hyderabad, Hyderabad 500046, India

\*Author for correspondence (sdsp@uohyd.ernet.in)

MS received 17 August 2019; accepted 24 November 2019

**Abstract.** We report experimental studies on the self-assembly of silica microspheres and Laponite nanoplatelets (NPs) in evaporating sessile droplets and in thin films, respectively. A ring-like stain of the silica microspheres with positional order is observed after the evaporation of sessile droplets due to the coffee-ring effect. This effect is suppressed in the binary mixtures of silica microspheres and Laponite NPs. A depletion zone has been observed in the mixtures during the sessile droplet evaporation, the width of which can be tuned by varying the compositions. We demonstrate a simple method for preparing core-shell particles by evaporating thin films of binary mixtures in which the Laponite NPs self-assemble to form a crystalline shell on the amorphous silica microspheres. We present a possible orientation of the Laponite NPs in the shell.

**Keywords.** Self-assembly; micro and nanoparticles; depletion zone; evaporation; core-shell particles.

## 1. Introduction

The self-assembly of micro- and nano-sized objects into larger structures is a subject of immense interest in the field of material science [1–3]. In case of anisotropic nanoparticles such as the nanoplatelets (NPs), the self-assembly and phase behaviour are very different than that of the spherical nanoparticles [4–8]. The self-assembly of colloidal particles, driven by evaporation, exhibits several complex phenomena. One such intricate phenomenon is the *coffee-ring effect* in which a pattern of dispersed particles is left out by the droplets when they are evaporated from a solid surface [9–12]. For a given suspension, the wetting properties of the substrate dictate the pattern and the final structure of the deposits.

The evaporation of sessile droplets and films have been studied due to its relevance in industrial applications such as printing, painting, coatings and films [13–17]. Suspended particles in the droplets are transported towards the periphery, while drying, due to the radial capillary flow, the so-called Marangoni flow; as a consequence stains are formed which are undesirable in many applications. There have been various efforts to suppress the stain formation. For example Shi *et al* [18] used hydrophobic fumed silica in an evaporating ethanol/water droplet that suppresses the capillary flow and leads to a uniform deposits. Talbot *et al* [19] used Laponite NPs to control the radial flow inside the picolitre droplets to produce uniform deposit. They argued that this effect is due to the sol-gel transition of Laponite during the evaporation. Liu *et al* [20] prepared supraparticles using

bi-disperse colloidal aqueous suspensions, where the smaller colloids mostly self-assemble into ordered structures at the periphery. Recently, we reported artificial nacre-like structures produced by evaporation of Laponite NP suspensions [21]. So far, drying experiments are mostly focused on spherical nano or microparticles in different suspension geometries. Such studies in the binary mixture consisting of microspheres and NPs are largely unexplored. In this paper, we present some preliminary and new results on drying experiments, of sessile droplets and thin films of binary suspensions consisting of silica microspheres and Laponite NPs. Our results include a novel method for preparing core-shell particles where the shell is a crystalline film on the amorphous silica core.

## 2. Methods and materials

Laponite is a plate-like charged silicate of average diameter 25 nm and thickness 1 nm [5]. They are available in the powder form which is used in this study. They were used without further purification. The powder is dissolved in a desired amount in milliQ water and mixed thoroughly by using magnetic stirrer for 2 h, followed by sonication for about 10 min for breaking any clusters present in the dispersion [22]. The binary mixtures of Laponite with monodispersed silica microspheres of diameters ranging from 1.2 to 8  $\mu\text{m}$ , are prepared by mixing the stock solutions of individual suspension. Concentration of the microspheres varied from 0.1 to 2 wt% and

the platelet concentration varied from 0.1 to 3 wt%. Zeta potentials of the Laponite and microspheres are  $-40$  and  $-75$  mV, respectively. Sessile droplets or thin films of the

mixture are prepared on hydrophilic glass plates. We used  $10\ \mu\text{l}$  for the sessile droplet and  $50\ \mu\text{l}$  for the thin film experiments. The droplets or films are dried at an ambient

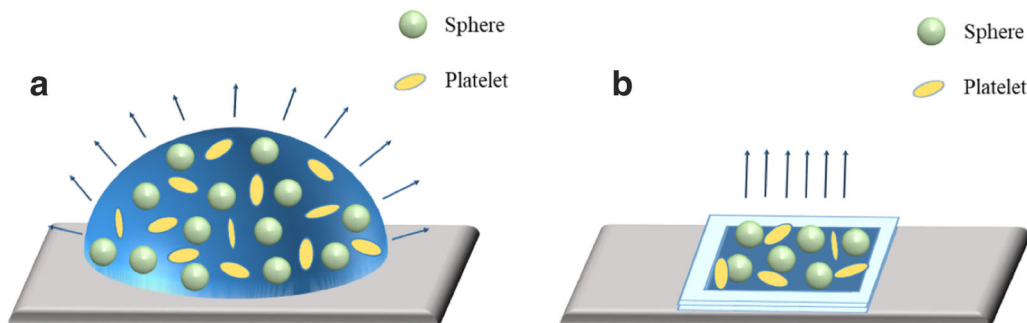


**Figure 1.** Schematic overview of suspension geometries for evaporation. Evaporation of (a) sessile droplet and (b) thin film ( $5 \times 5\ \text{mm}^2$ ). Silica microparticles (sphere) and Laponite NPs (platelet) are uniformly suspended in milliQ water. Arrows indicate the direction of evaporation.

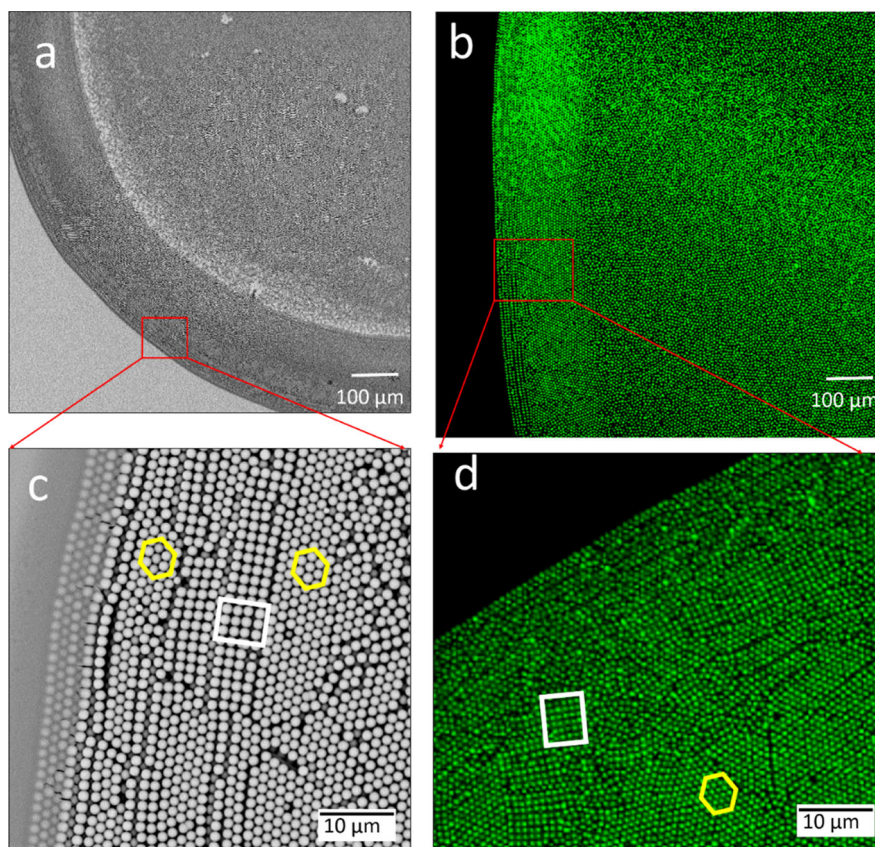


**Figure 2.** Deposition patterns obtained from a sessile dried droplet. The droplet is prepared from the solution state in which 0.5 wt% of silica microsphere (diameter  $1.2\ \mu\text{m}$ ) is dispersed. (a) Scanning electron microscope (SEM) and (b) confocal images of ring-shaped stain of the sessile droplet left on the substrate after evaporation. (c, d) A close-up view of the stains. Square and hexagonal ordering are indicated in yellow and white, respectively.

temperature of 25°C and relative humidity of 50%. In case of film drying, the glass plates are partially covered to prevent contamination due to airborne debris and to slow down the evaporation. The dried samples are studied using a high-resolution FESEM (Carl Zeiss Ultra 55) and confocal microscope (Leica SP8) with an oil immersion objective. Optical and birefringence imaging is done using a polarizing optical microscope (Olympus BX51) and a first-order retardation plate, also known as  $\lambda$ -plate (retardation of 530 nm).

### 3. Results and discussion

In this study, we used two types of suspension geometries namely, the sessile droplets and the thin films in a confined area ( $5 \times 5 \text{ mm}^2$ ). Figure 1 shows the schematic overview of the two suspension geometries. Evaporation in sessile

droplets takes place in all directions, whereas in thin films it occurs in the vertical direction.

#### 3.1 Ring-shaped colloidal stains from sessile droplets

Our study begins with the investigation on sessile droplets in which spherical particles of diameter  $1.2 \mu\text{m}$  are dispersed in milliQ water. When the water from the droplet is completely evaporated, the particles are deposited on the substrate. Figure 2a and b shows scanning electron microscope (SEM) and confocal images of deposition near the edge. The deposition is not uniform throughout the area. A close-up view by SEM (figure 2c) and confocal microscope (figure 2d) shows that the density of the deposited particles is larger in a ring-shaped stain at the edge due to the so-called coffee-ring effect. A structural change from ordered to disordered

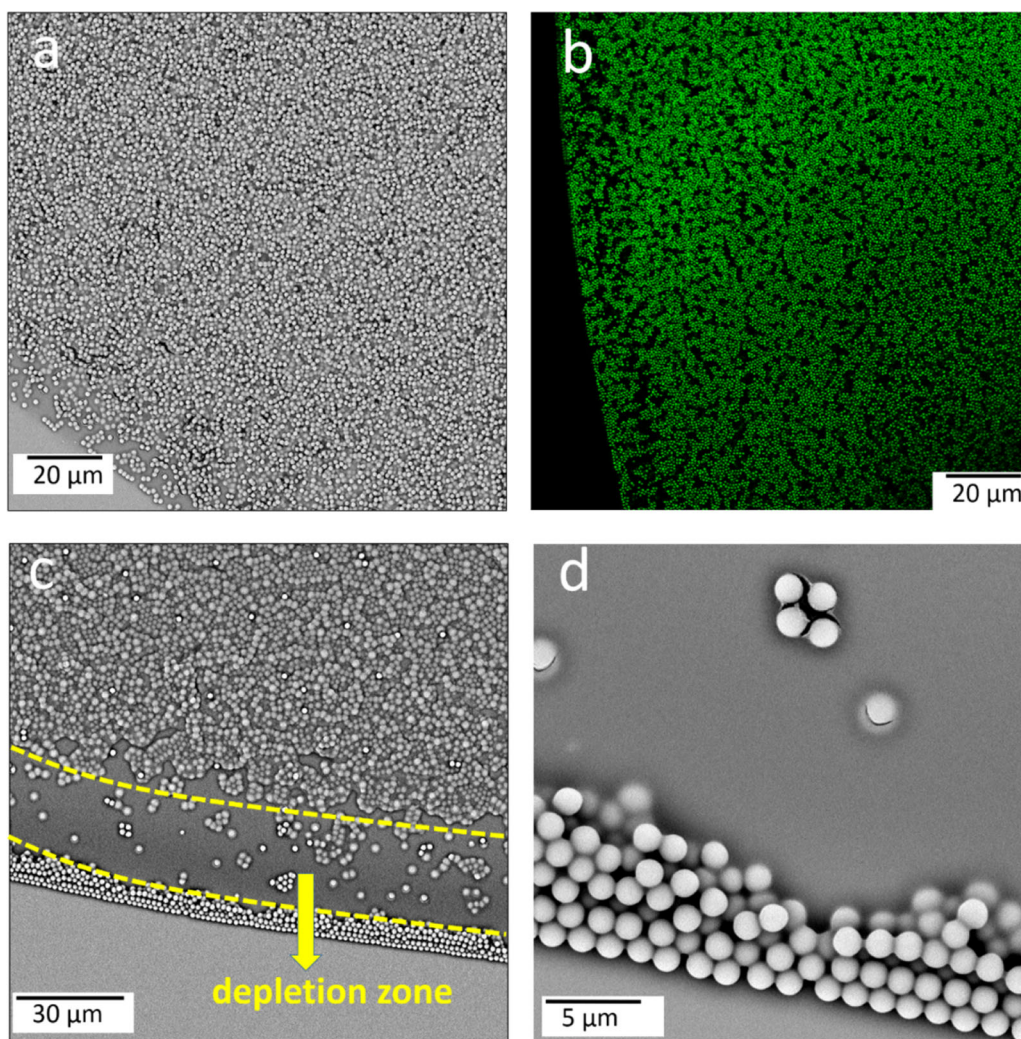


**Figure 3.** (a, c, d) Scanning electron microscopy and (b) confocal images of a dried droplet consisting of silica microspheres (diameter  $1.2 \mu\text{m}$ ) and Laponite NPs. Concentration of microspheres is 1 wt% and Laponite concentration is 1 wt% in (a, b) and 0.5 wt% in (c, d). (c) An annular-ring-like depletion zone ( $\sim 30 \mu\text{m}$ ) is observed near the periphery of the stain. (d) A close-up view of the depletion zone.

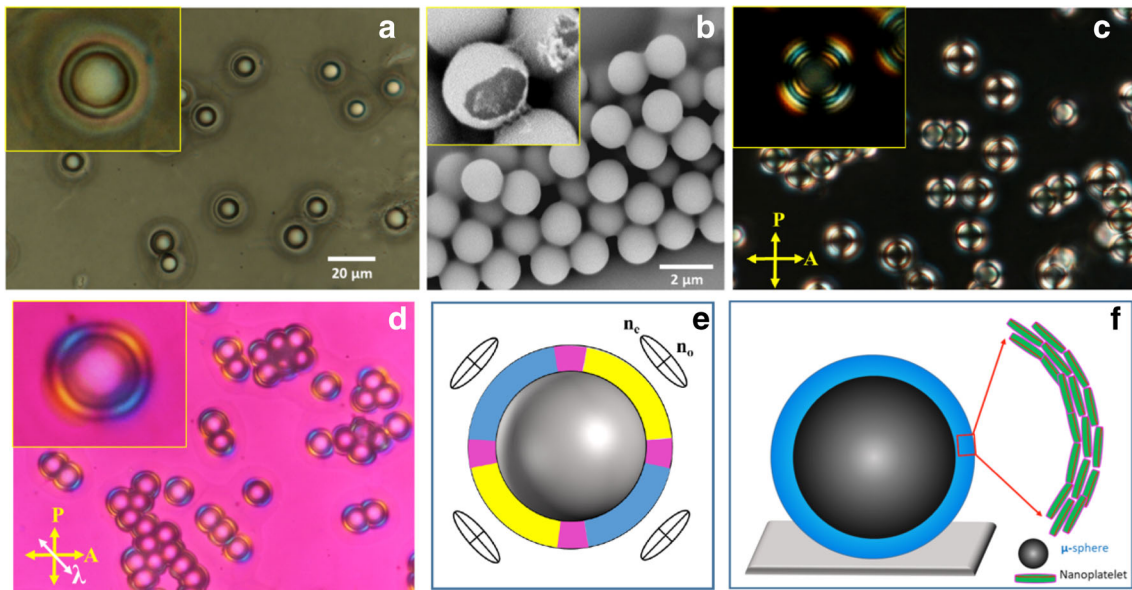


**Figure 4.** Core-shell microparticles prepared by evaporating thin films. **(a)** Light microscope image of silica particles (diameter  $8\ \mu\text{m}$ ) after drying. **(b)** FESEM image of the core-shell silica particles (diameter  $1.2\ \mu\text{m}$ ) with shell thickness  $\sim 200\ \text{nm}$ . The inset shows microparticles with broken shell. **(c)** Light microscope image taken between a crossed polarizer (P) and analyser (A). **(d)** Image after inserting a  $\lambda$ -plate, fast axis oriented at  $45^\circ$  with respect to the polarizer. **(e)** Refractive index ellipsoids corresponding to blue and yellow regions. Extraordinary ( $n_e$ ) and ordinary ( $n_o$ ) refractive indices are labelled. **(f)** Schematic orientation of the Laponite NPs in the shell.

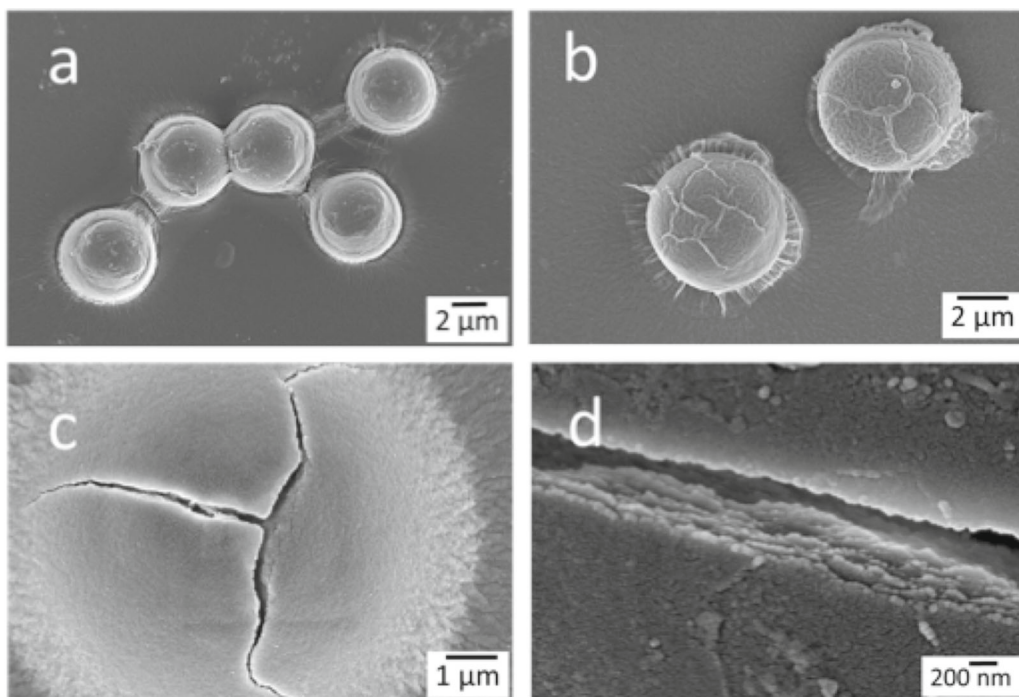


**Figure 5.** Effect of coating thickness on the silica microspheres. **(a, b)** SEM image of a few microspheres showing rough shell surface after third coating. **(c)** Crack formation on the shell. **(d)** A close-up view of a crack showing a nacre-like structure of the shell.

state is observed as we move from the edge of the ring to the centre. In particular, closer to the edge of the stain a hexagonal order is found, followed by square and again hexagonal order, respectively. The positional order is destroyed as we move towards the centre of the ring. This kind of structural transition was also observed by Marín *et al* [23]. They showed that this transition originates from a temporal singularity of the flow velocity inside the evaporating droplets. When the deposition speed is low, that happens at the beginning of the evaporation, the particles have enough time to get arranged due to the Brownian motion, whereas towards the end, the speed of the particles is high enough that they get jammed into a disordered state.

### 3.2 Suppression of coffee-ring effect and formation of depletion zone

As a next step, we have studied the effect of Laponite NPs on the coffee ring. It is observed that the addition of Laponite NPs suppresses the formation of a coffee ring. For concentrations  $> 1$  wt% of both silica microparticles and Laponite, it forms nearly a uniform deposition of the silica particles as shown in figure 3a and b. At lower concentrations ( $< 1$  wt%), formation of an annular ring-like region near the edge is observed where the silica microspheres are mostly depleted (figure 3c). A close-up view of the depletion zone is shown in figure 3d. The width of the depletion zone grows with time and reaches a maximum when the evaporation is completed. Similar depletion zones near the periphery have been observed in systems of colloidal suspension containing surfactant molecules and in mixtures of polystyrene and poly(N-isopropylacrylamide) (pNIPAM) [20,24–27]. The formation of depletion zone is due to the inhomogeneous adsorption of the colloidal particles at the water–vapour interface which sets up the solutal Marangoni flow along the interface during the evaporation.

### 3.3 Formation of core–shell colloidal particles

In what follows, we present a method for the preparation of core–shell particles in which the Laponite NPs are deposited uniformly, making a thin shell on the surface of the silica microparticles. The core–shell particles are prepared in two ways. In the first approach, the micron-sized silica particles are spread and dried on the hydrophilic glass substrates and then the suspension of Laponite NPs is poured on to it and dried. In the second approach, the silica microspheres and Laponite NPs are mixed thoroughly and then drop casted on the hydrophilic substrates. In both cases the evaporation takes place vertically as shown in figure 1b, consequently there is no formation of the coffee ring. In the latter approach, the microspheres sediment under the gravity and then the NPs self-assemble on the surface of the silica microparticles to minimize the surface energy. The second approach is found to be more efficient as the coating is more uniform than the first one (figure 4a). Figure 4b shows the SEM image of a few core–shell particles of diameter  $8\ \mu\text{m}$ . The thickness of the

shell is uniform (see broken shell in inset of figure 4b) and the surface is highly smooth. The shell thickness depends on the concentration of the NPs and for 1 wt% it is about 200 nm on the silica particles of diameter  $1.2\ \mu\text{m}$ .

To explore the microstructure and properties of the shell, we looked at the core–shell particles between two crossed polarizers under the light microscope. Figure 4c shows the concentric and colourful interference rings surrounding the spherical microparticles with four crossed extinction directions (better seen in the inset of figure 4c). This clearly indicates that the shell is optically birefringent, possessing ordinary and extraordinary refractive indices. It means the shell has crystalline order. To get a qualitative idea about the retardation, we inserted a first-order waveplate ( $\lambda$ -plate retardation of 530 nm) with fast axis oriented at  $45^\circ$  with respect to the polarizer. According to the Michel–Levy chart, different colours represent different magnitudes of retardation across the sample [27]. For example, the background magenta colour indicates the region of minimum or zero retardation. The retardation of second-order blue is higher than the first-order yellow region. These two colours exchange places when the fast axis is rotated by  $90^\circ$ . This means that the long axis of the ellipsoid of index of the shell is parallel to the surface of the microspheres, as shown schematically in figure 4e. Based on the orientation of index of ellipsoid it is easy to comprehend that during the drying process, the Laponite NPs are deposited on to the surface of the microspheres as shown in figure 4f. In the shell, the NPs possess an orientational order with an average direction of orientation of the short axes of the NPs being perpendicular to the surface of the microspheres. The thickness of the shell can be enhanced by adding multiple coatings. For this purpose, the successive coatings are made each time after drying the sample completely. However, after second coating the deposition is not uniform as a result of which the surface becomes rough (figure 5a and b). In addition, cracks are formed as shown in figure 5c. A close-up view of the cracks reveals an artificial nacre-like structure of the film (figure 5d), as reported previously [21].

## 4. Conclusion

After the evaporation of sessile droplets, the silica microspheres form a narrow ring-like zone where the particles are self-assembled due to the coffee-ring effect. The addition of Laponite NPs suppresses the coffee-ring effect and forms a uniform deposit at higher concentrations and a narrow depletion zone at lower concentrations. A valuable bonus of our studies is a simple method for preparing core–shell particles in which the shell is crystalline. The Laponite NPs are spontaneously self-assembled, forming a shell upon drying and exhibit crystalline order. We have proposed an orientation of the Laponite NPs in the shell. Such core–shell particles could be useful as markers or tracer particles for various applications.

## Acknowledgements

RKP acknowledges the support from the Department of Science and Technology, India for an INSPIRE Faculty Award Grant (DST/INSPIRE/04/2016/002370). SD gratefully acknowledges the support from the DST (DST/SJF/PSA-02/2014-2015) and SERB. DVS acknowledges DST for INSPIRE fellowship.

## References

- [1] Nie Z, Petukhova A and Kumacheva E 2010 *Nat. Nanotechnol.* **5** 15
- [2] Glotzer S C and Solomon M J 2007 *Nat. Mater.* **6** 557
- [3] Abécassis B, Tessier M D, Davidson P and Dubertret B 2014 *Nano Lett.* **14** 710
- [4] Sacanna S, Korpics M, Rodriguez K, Colón-Meléndez L, Kim S H, Pine D J *et al* 2013. *Nat. Commun.* **4** 1688
- [5] Pujala R K 2014 *Dispersion stability, microstructure and phase transition of anisotropic nanodiscs* (Switzerland: Springer International Publishing). ISBN 978-3-319-04555-9, <https://doi.org/10.1007/978-3-319-04555-9>
- [6] Kuijk A, van Blaaderen A and Imhof A 2011 *J. Am. Chem. Soc.* **133** 2346
- [7] Ruzicka B, Zaccarelli E, Zulian L, Angelini R, Sztucki M, Moussaïd A *et al* 2011 *Nat. Mater.* **10** 56
- [8] Zhang Z and Glotzer S C 2004 *Nano Lett.* **4** 1407
- [9] Mampallil D 2014 *Reson.—J. Sci. Educ.* **19** 123
- [10] Deegan R D, Bakajin O, Dupont T F, Huber G, Nagel S R and Witten T A 2000 *Phys. Rev. E* **62** 756
- [11] Deegan R D, Olgica B, Dupont T F, Greg H, Nagel S R and Thomas A W 1997 *Nature* **389** 827
- [12] Mampallil D and Eral H B 2018 *Adv. Colloid Interface Sci.* **252** 38
- [13] Bigioni T P, Lin X M, Nguyen T T, Corwin E I, Witten T A and Jaeger H M 2006 *Nat. Mater.* **5** 265
- [14] Brinker C J, Lu Y, Sellinger A and Fan A 1999 *Adv. Mater.* **11** 579
- [15] Zhang L, Liu H T, Zhao Y, Sun X N, Wen Y G, Guo Y L *et al* 2012 *Adv. Mater.* **24** 436
- [16] de Gans B J and Schubert U S 2004 *Langmuir* **20** 7789
- [17] Dugas V, Broutin J and Souteyrand E 2005 *Langmuir* **21** 9130
- [18] Shi J, Yang L and Bain C D 2019 *ACS Appl. Mater. Interfaces* **11** 14275
- [19] Talbot E L, Yang L, Berson A and Bain C D 2014 *ACS Appl. Mater. Interfaces* **6** 9572
- [20] Liu W, Midya J, Kappl M, Butt H J and Nikoubashman A 2019 *ACS Nano* **13** 4972
- [21] Pujala R K, Kumar M P and Dhara S 2018 *J. Phys. D: Appl. Phys.* **51** 304003
- [22] Pujala R K, Schneijdenberg C T W M, van Blaaderen A and Bohidar H B 2019 *Sci. Rep.* **8** 5589
- [23] Marín Á G, Gelderblom H, Lohse D and Snoeijer J H 2011 *Phys. Rev. Lett.* **107** 085502
- [24] Still T, Yunker P J and Yodh A G 2012 *Langmuir* **28** 4984
- [25] Varanakkottu S N, Anyfantakis M, Morel M, Rudiuk S and Baigl D 2015 *Nano Lett.* **16** 644
- [26] Mayarani M, Basavaraj M G and Satapathy D K 2019 *Soft Matter* **15** 4170
- [27] Olympus Scientific Solutions: <https://www.olympus-lifescience.com/en/microscoperesource/primer/techniques/polarized/fir-storderplate/>